Defect Structure of Irradiated Graphite Depending on The Incident Angle of Neutrons: A Molecular Dynamics Study

Jiho Kim[a], Kunok Chang[a*]
[a]*Department of Nuclear Engineering, Kyunghee University, Yongin, Republic of Korea*
[*]*Corresponding author: kunok.chang@khu.ac.kr*

1. Introduction

Graphite is broadly used in nuclear reactor as moderator and reflector. For the case of AGN-201K, which is a nuclear reactor for educational purpose, graphite is used as reflector and it is exposed to the fast neutrons. Therefore, predicting the irradiation damage of graphite by high-speed neutrons is very important in evaluating the aging deterioration of AGN-201K. In this study, a defect structure due to the neutron irradiation damage of graphite was predicted using a simulation technique.

We simulated atomistic behavior of graphite after during the neutron irradiation by using a Large-scale Atomic/Molecular Massively Parallel Simulator (LAMMPS), an open-source program to perform a Molecular Dynamic (MD) simulation, to simulate the evolution of the defect structure of irradiated graphite.

2. Physics of Simulation

2.1 Potential of System

Selection of the interatomic potential is a key task for reliable molecular dynamics simulations.

Adaptive Intermolecular Reactive Empirical Band Order (AIREBO) potential is used for the chemical and intermolecular interactions of graphite [1]. Moreover, it can depict the interlayer relationship, which can happen during neutron irradiation.

2.2 Binary Elastic-Collision Dynamics (BECD)

To simulate the neutron irradiation, we applied the BECD on LAMMPS. Assuming that the incident particle travels along the z-axis and collides elastically with the carbon atom that located at the origin.

In Fig 1, the orange vector represents the incident neutron, the purple vector represents the recoiled neutron, and the blue one represents the recoiled carbon atom.

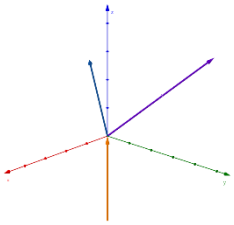

Fig. 1 Example of BECD, each vector has speed and direction

Since the process is elastic collision, the kinetic energy and momentum of the process should be conserved. Using the conservation of momentum and energy, we can get equation (1), (2), (3), and (4). The subscript n, C, i, f, x, y, and z denotes neutron, carbon, before collision state, after collision state, x, y, and z directions.

$$\frac{1}{2}\mathrm{m_n}v_{ni}^2 = \frac{1}{2}m_n v_{nf}^2 + \frac{1}{2}m_C v_{Cf}^2 \quad (1)$$
$$0 = \mathrm{m_n}v_{nfx} + \mathrm{m_C}v_{Cfx} \quad (2)$$
$$0 = \mathrm{m_n}v_{nfy} + m_C v_{Cfy} \quad (3)$$
$$\mathrm{m_n}v_{ni} = m_n v_{nfz} + m_C v_{Cfz} \quad (4)$$

Divide equation (1) to (4) with $\mathrm{m_1}$ and set M as $\mathrm{m_n}/m_C$. After, some calculus, we can get equation (5) to (8).

$$\mathrm{v_{ni}^2} = v_{nf}^2 + Mv_{Cf}^2 \quad (5)$$
$$\mathrm{v_{nfx}} + \mathrm{Mv_{Cfx}} = 0 \quad (6)$$
$$\mathrm{v_{nfy}} + Mv_{Cfy} = 0 \quad (7)$$
$$\mathrm{v_{nfz}} + Mv_{Cfz} = \mathrm{v_{ni}} \quad (8)$$

By adding the square of equation (5), (6), and (7), we can get equation (9)

$$\mathrm{v_{nf}^2} + 2M\left(v_{nfx}v_{Cfx} + v_{nfy}v_{Cfy} + v_{nfz}v_{Cfz}\right) + M^2 v_{Cf}^2 = v_{ni}^2 \quad (9)$$

Substituting equation (5) to the LHS of equation (9), and replacing $\mathrm{v_{nfx}}$, $\mathrm{v_{nfy}}$, and $\mathrm{v_{nfz}}$ with equation (6) to (8). As a result, we can derive equation (10).

$$2\left\{-\mathrm{Mv_{Cfx}^2} - Mv_{Cfy}^2 + \left(v_{ni} - Mv_{Cfz}\right)v_{Cfx}\right\} = (1 - M)v_{Cf}^2 \quad (\because \mathrm{v^2} = v_x^2 + v_y^2 + v_z^2) \quad (10)$$

With some calculation and spherical coordinate system, $\mathrm{v_{Cfz}} = v_{Cf}\cos\theta_C$, we finally get equation (11).

$$\mathrm{v_{Cf}} = \frac{2cos\theta_C}{1+M}\mathrm{v_{ni}} \quad (11)$$

We now derive the relationship between the incident neutron's speed and recoiled carbon atom's speed. The atom that collide with incoming neutron is called as 'Primary Knock-on Atom', or PKA.

By using equation (11), the energy relation of PKA and incident neutron derived as equation (12)

$$\mathrm{E_{PKA}} = \Lambda \mathrm{E_{incident}}\cos^2\theta_C \quad (12)$$
$$\Lambda = \frac{4\mathrm{m_n}m_C}{(m_n+m_C)^2} \quad (13)$$

From equation (12), it is obvious that the PKA energy decreases when they recoiled to other direction rather than the head-on collision, or $\theta_C = 0$.

2.3 Simulation Basics

We simulate 16320 carbon atoms in the rectangular area with 8.3×5.1×3.125 nm. The boundary condition was set as periodic condition for whole directions. We use perfect AB-stacked graphite.

In the LAMMPS, the incident energy does not matter to the simulation. Only the PKA energy and direction of the PKA are the variable of the situation. For example, when PKA energy is 100 eV and direction of PKA is Θ=30˚, we cannot distinguish it whether it is originated by 352 eV neutron with head-on collision or 469 eV neutron passed through the z-axis and recoiled to given direction.

Therefore, to simplify the simulation condition, we assumed the most conservative condition, a head-on collision.

Besides, we consider that the different recoiled angle of PKA with same energy affects differently to the system. Therefore, we set three variables, PKA energy, Θ and Φ as Fig. 2. In this figure, the red atom at bottom-left is the PKA. Later, we denote these variables as $<E_{PKA}, \Theta, \Phi>$

A recoiled polar and azimuthal angle of the carbon atom, Θ and Φ, generated by the head-on collision, are defined in standard spherical coordinate as illustrated in Fig. 3.

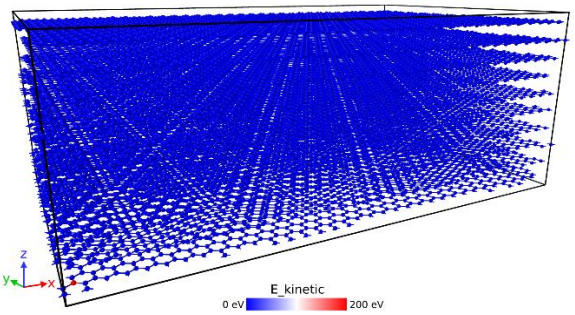

Fig. 2. Graphite simulation cell in LAMMPS: red atom at the bottom left is a PKA atom right after the collision

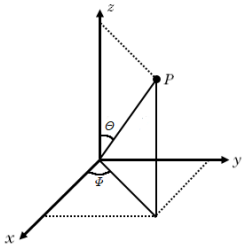

Fig. 3. Angle definition

Before the collision, we applied thermal state to system with NpT ensemble, and then put the system in the 300K for about 0.1 ps. After thermal equilibrium, collision process was conducted with NVE ensemble.

3. Results

We simulated for various PKA energy and recoiled angle. The defect structure found from each condition is tabulated as Table I. We colored the cell with green when the defects do not contain vacancies.

Angle (˚)		PKA Energy (eV)						
Θ	Φ	10	25	50	75	100	150	200
0	0	X	TT	R	TT	TT	TT	G
30	0	X	TT	FP	TT	D	G,II,TT	TT
	30	X	TT	R	II,TT	II	TT	G,TT
	60	X	TT	FP	FD	C,TT	II,TT	II,TT
	90	X	TT	TT	G	TT	G	C
60	0	X	R	TT	TT	G	II,TT	G,TT
	30	X	R	BB	C,TT	TT	G	G,TT
	60	X	R	BB	G	II	D,TT	G,TT
	90	X	R	R	G	G	D	G,TT
90	0	X	R	R	R	R	R	SW
	30	X	R	R	G	G	G	SW
	60	X	R	R	R	Dis	G	G
	90	X	R	R	R	R	SW	R

Table I: Simulation results - X: No reaction | R: Recovered | SW: Stone-Wales defect | Dis: dislocation | Single-interstitial: G, D | Di-interstitial: C, TT, BB, FD | Uncolored: Include vacancies

In Table I, each interstitial defects are nomenclated and illustrated as Fig. 4 by Gulans et al. [2], who simulated the structural defects with the Density Function Theory (DFT) for a self-diffusion of carbon atom in bilayer graphite. Additionally, we use other abbreviations X, R, and II, which stands for no reaction, recovered, and interlayer interstitials.

Difference between the term X and R, it is determined by the PKA's first interaction with other carbon atom. The X do not strike with other atom rather R generates secondary knock-on atoms but recovered to original condition.

Fig. 5 to 8 are the final time step of the simulation, which is 6.65~6.67 ps after the whole process.

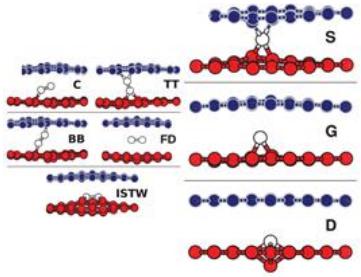

Fig. 4. Graphite interstitial defects

Gulans et al. conducted the calculation to find the graphite defects with the self-diffusion system [2], rather than the neutron-graphite irradiation process. From this difference, we found that the previous study performed by them yield slight displacement of carbon atoms while we found significant deformation of graphite layer in Fig.

5 to 8. These deformations are originated by the kinetic energy of the PKA.

3.1 Representative Results for Each Defects

In Fig. 5, the PKA drags one upper layer atom to form the TT defect. Unlike the other simulations, the defect structure itself stabilized while it excites the ambient atoms. During this process, atoms around those two defected atoms lose its potential energy up to -7.2 eV when the normal graphite's potential energy is -7.6 eV. Other TT defects generated by 25 eV PKA shows similar results.

Fig. 7 shows both II, TT, and vacancies. The green-colored atom is an II atom with low potential energy. Due to its instability, it floats between the layers of graphite before it interacts with other atoms. In this case, we simulates the same process with more time-step, 30000 steps or about 68 ps. Despite the increase of time-step, the II atoms does not bond with other atoms. Plus, the vacancies generated by PKA excite the ambient atoms, so some of them have lower potential energy than others.

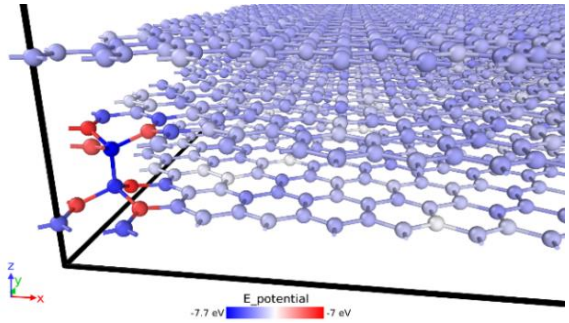

Fig. 5. <25 eV, 30˚, 60˚> case (TT)

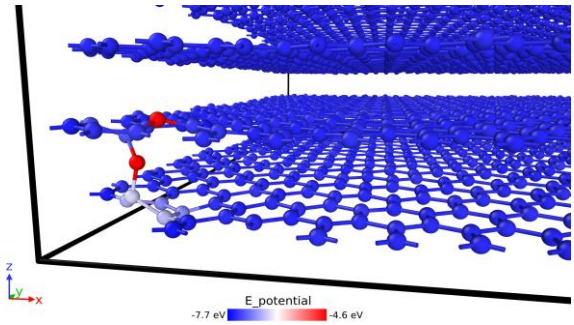

Fig. 6. <50 eV, 60˚, 30˚> case (BB)

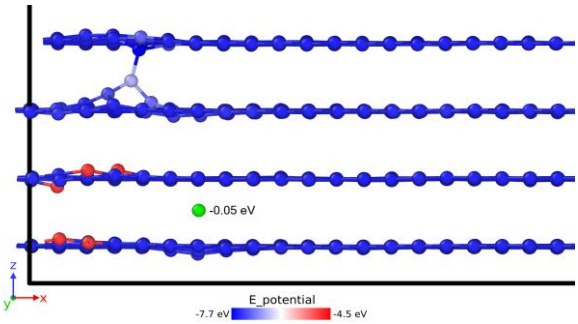

Fig. 7. <75 eV, 30˚, 30˚> case (II+TT)

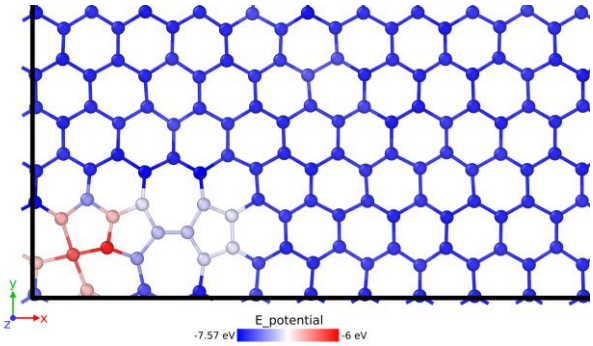

Fig. 8. <200eV, 90˚, 30˚> case (SW); two 5-7 polygons cluster

The Stone-Wales defect (SW) [3] is a unique defect structure shown in graphite. It has two pentagons and heptagons that combined along the heptagon's edge. From the MD simulation, it was found only when the PKA moves parallel to the graphite layer like Fig. 8. It has lower potential energy than ambient atoms. Owing to another defect structure which formed by a pentagonal shape next to the left side of SW defect, the SW defect stabilized while the additional pentagonal defect got lower potential energy.

Recent study suggests that the E_d is about 25 eV for graphite [4]. Simulation result reached to the expected value. As we can check on the Table I, the PKA theory is validated since the PKA with $2E_d$ (50 eV) somehow recoiled with other carbon atom whether a defect formed or not.

4. Conclusion

The major finding was the fact that the angle of the PKA is a crucial variable that can affect the type of the defect structure as shown in Table I when the simulation has same incident neutron energy and PKA energy. It is more likely to form a defect when the polar angle (Θ) of PKA is smaller, or PKA moves toward the upper layer of graphite. These phenomena can be checked at the low energy regions, for instance, 25 eV and 50 eV cases in Table I.

It is due to the low van der Waals force between the layers of graphite. When the van der Waals force act on the PKA is smaller, it can collide with other atoms with more energy to make a defect.

We got more specific defect structures than the DFT calculation results. DFT provides only one structure sets, for example, single-interstitial group S,G, and D, or di-interstitial group C, TT, BB, FD, and ISTW, for each simulation [2]. However, MD provides various types of defect structures simultaneously at the high-level PKA energy situations. The 100 eV to 200 eV region in Table I, such as <150 eV, 30˚, 0˚>, represent these phenomena.

The main factor to achieve this was an implementation of neutron irradiation as an elastic collision to the simulation process. Finally, we can use MD to simulate the irradiation of materials induced by neutron.

REFERENCES

[1] Steven J. Stuart, Alan B. Tutein and Judith A. Harrison, A Reactive Potential for Hydrocarbons with Intermolecular Interactions, Journal of Chemical Physics, Vol. 112, pp. 6472-6486, 2000.
[2] Andris Gulans, et al., Bound and Free Self-Interstitial Defects in Graphite and Bilayer Graphene: A Computational Study, Physical Review B, Vol. 84, p. 024114
[3] A.J Stone and D.J. Wales, Theoretical Studies of Icosahedral C_{60} and Some Related Species, Chemical Physics Letters, Vol. 128, pp. 501-503, 1986.
[4] A.J McKenna, et al., Threshold Displacement Energy and Damage Function in Graphite from Molecular Dynamics, Carbon, Vol. 99, pp. 71-78, 2016.